An ab Initio Study of the Mechanism of the Atherton–Todd Reaction between Dimethyl Phosphonate and Chloro- and Fluoro-Substituted Methanes

Emil M. Georgiev,[1a] Jose Kaneti,[1b] Koljo Troev,[1c] and D. Max Roundhill*,[1a]

Contribution from the Department of Chemistry, Tulane University, New Orleans, Louisiana 70118, and The Institutes of Polymers and Organic Chemistry, Bulgarian Academy of Sciences, Sofia, Bulgaria

Received March 24, 1993®

Abstract: A new mechanism for the amine promoted Atherton–Todd reaction is proposed, based on an ab initio theoretical study of alternative reaction pathways. Conformational analyses have been performed on a set of model phosphorus-containing species, including dimethyl phosphonate, $(CH_3O)_2P(O)H$, dimethyl chlorophosphate, $(CH_3O)_2P(O)Cl$, monomethyl phosphonate, $(CH_3O)(HO)P(O)H$, and its anion, $[(CH_3O)PHOO]^-$ phosphonic acid, $(HO)_2P(O)H$, and its anion, $[(HO)PHOO]^-$, dimethyl phosphite, $(CH_3O)_2POH$, and its anion, $[(CH_3O)_2PO]^-$, as well as the anions of monomethyl phosphite, $[(CH_3O)(HO)PO]^-$, and phosphorous acid, $[(HO)_2PO]^-$. In addition a series of chloro- and fluoro-substituted methanes $CCl_{4-n}F_n$, their hydrogen derivatives $CHCl_{3-n}F_n$, and their corresponding anions $[CCl_{3-n}F_n]^-$, for $n = 0, 1, 2$, have also been computed. Computations have also been carried out on NH_3, NH_4^+, and $CH_3NH_3^+$. Reaction pathways which correspond to the different possible steps in the mechanism of the Atherton–Todd reaction have been theoretically explored involving the location of a number of transition structures. The geometries of the studied systems have been fully optimized with the 6-31+G* basis set, whereas frozen-core Møller–Plesset (MP2) perturbation theory has been applied to correct for correlation effects. Frequency calculations have been performed at HF/6-31+G* on the optimized structures in order to ascertain the type of the located stationary points and to obtain the corresponding zero point energies. The computational results provide an explanation for the experimentally observed order of reactivity of dimethyl phosphonate toward different chloro- and fluoro-substituted methanes under the Atherton–Todd reaction conditions.

Introduction

The chemistry of the phosphorus compounds has received much theoretical attention in the recent years mainly because of the significant role that phosphorus esters play in biological systems. The diesters of phosphonic acids occupy an important position in organophosphorus chemistry since they are frequently intermediates in the synthesis of a variety of biologically active species including organophosphates, amidophosphates, and linear polyphosphates. With respect to introducing these functionalities into biomolecules, the Atherton–Todd reaction is a useful synthetic approach. It involves the oxidation of dialkyl phosphonates with chlorocarbons into dialkyl or trialkyl phosphates under mild conditions.[2] The versatility of the reaction results from the fact that the initial products in the reaction are the highly reactive dialkyl chlorophosphates (eq 1), which in the presence of amines

$$RO\text{–}\overset{\overset{O}{\|}}{\underset{\underset{H}{|}}{P}}\text{–}OR + CCl_4 \xrightarrow{\text{Base}} RO\text{–}\overset{\overset{O}{\|}}{\underset{\underset{Cl}{|}}{P}}\text{–}OR + CHCl_3 \qquad (1)$$

or alcohols are converted *in situ* into the corresponding dialkyl phosphoramides or trialkyl phosphates, respectively. One important new area of application for the Atherton–Todd reaction, which was recently explored by Brosse and co-workers,[2c] is the immobilization of pharmacologically active amines onto linear polyphosphonates, thereby yielding a new class of biodegradable and bioresorbable polyamidophosphates.

The commonly accepted mechanism for the Atherton–Todd reaction[3-5] is based primarily on the early kinetic investigations by Steinberg.[3] The initial step of this mechanism involves deprotonation of the dialkyl phosphonate $(RO)_2PH(O)$ by a base **B** to give the dialkyl phosphite anion, $(RO)_2P(O)^-$. This dialkyl phosphite anion then reacts as a nucleophile toward carbon tetrachloride, resulting in the sequence of reactions shown in Scheme I:

Scheme I

$$(RO)_2P(O)H + B \rightarrow (RO)_2P(O)^- + (HB)^+$$

$$(RO)_2P(O)^- + CCl_4 \rightarrow (RO)_2P(O)Cl + CCl_3^-$$

$$CCl_3^- + (RO)_2P(O)H \rightarrow HCCl_3 + (RO)_2P(O)^-$$

This initial step is also generally proposed as a common one for all of the different addition reactions of dialkyl hydrogen phosphonates which results in cleavage of the P–H bond.[6] In this scheme, step 1 leads to the formation of the catalytically active species $(RO)_2PO^-$, while steps 2 and 3 in the scheme represent the catalytic cycle of reactions that lead to the formation of products. Within this catalytic cycle of reactions, dialkyl phosphonate and carbon tetrachloride react to form dialkyl chlorophosphate and chloroform as the final products of the Atherton–Todd reaction. A simple equilibrium shift toward the dialkyl phosphite tautomer[4] in step 1 and the formation of pentacoordinated phosphorane intermediates in step 2[2] have also been discussed as variations in Scheme I.

* Abstract published in *Advance ACS Abstracts*, October 15, 1993.

(1) (a) Tulane University. (b) Institute of Organic Chemistry, Bulgarian Academy of Sciences. (c) Institute of Polymers, Bulgarian Academy of Sciences.

(2) (a) Atherton, F. R.; Openshaw, H. T.; Todd, A. R. *J. Chem. Soc.* **1945**, 660–3. (b) Atherton, F. R.; Todd, A. R. *J. Chem. Soc.* **1947**, 674–8. (c) Brosse, J.-C.; Derouet, D.; Fontaine, L.; Chairatanathavorn, S. *Makromol. Chem.* **1989**, *190*, 2339–2345.

(3) Steinberg, G. M. *J. Org. Chem.* **1950**, *15*, 637–47.

(4) Nifantiev, E. E.; Blagowestenskij, A. M.; Sokorenko, A. M.; Skljarskij, L. S. *Zh. Obshch. Khim.* **1974**, *44*, 108–10.

(5) Kong, A.; Engel, R. *Bull. Chem. Soc. Jpn.* **1985**, *58*, 3671–2.

(6) Nifantiev, E. E. *The Chemistry of the Hydrophosphoryl Compounds*, Mir: Moskow, 1983.

0002-7863/93/1515-10964$04.00/0

Tertiary, secondary, and primary amines are the most commonly used bases under the Atherton–Todd conditions.[2-5] The validity of the first step for the case of the base being an amine is, however, questionable, since it has been established that amines are alkylated and not protonated at the nitrogen by dialkyl phosphonates:[7]

$$(RO)_2P(O)H + NR'_3 \rightarrow [(RO)P(O)HO]^-[RNR'_3]^+ \quad (2)$$

The phosphorus-containing ammonium salts thus formed have been shown to exist in DMSO solution as the free ions.[7] Furthermore, we have recently demonstrated that alkylammonium or metal salts containing monoalkyl phosphonate anions also promote the Atherton–Todd reaction.[8] Taking into account the observation of Kong and Engel that the Atherton–Todd reaction does not take place in the absence of base,[5] these recent results indicate that the **monoalkyl** phosphonate anion is playing a key role as an intermediate in the amine-promoted Atherton–Todd reaction.

The Atherton–Todd reaction is one of a group of similar synthetic approaches that can be used to introduce the phosphonate group into polymers and biopolymers. Two other such reactions are those of Abramov and Pudovik.[9,10] The Abramov reaction involves the addition of a dialkyl phosphonate to a carbonyl group of an organic compound, and the Pudovik reaction involves the addition of a dialkyl phosphonate to an activated double bond. These two reactions, along with that of Atherton–Todd, involve cleavage of the P–H bond of the phosphonate. All three reactions are base-promoted, and all are proposed to have a common initial step that involves deprotonation of the dialkyl phosphonate, as shown in the first step of Scheme I. Because of the general importance of the reactivity of phosphonate anions as nucleophiles in reactions such as these, we have decided to use ab initio methods to theoretically explore some of the possible pathways for the Atherton–Todd reaction. We have chosen to carry out these calculations by searching the potential energy surface of a set of model compounds. We have used complete geometry optimization of all the critical points related to the energy minima and transition structures located along the reaction path using the standard 6-31G* basis sets, supplemented with diffuse functions on the heavy atoms, and including electron correlation at the second-order Møller–Plesset (MP2) level. The structures of dimethyl phosphonate and phosphonic acid have been the subject of previous theoretical studies by Van Wazer and Ewig. These authors have computed three conformers for dimethyl phosphonate by carrying out the conformational analysis with an STO-3G* basis set, while a 4-31G* basis set was applied for the optimization of the geometry of phosphonic acid.[11,12] No frequency calculations, which are essential for the determination of the type of the located critical points, were reported in these papers. Furthermore, the only calculations currently available in the literature are focused on addressing the ground-state geometries of these compounds, and no previous attempt has been made to calculate reaction pathways which involve these compounds.

Our primary interest in these proton-transfer reactions involving dialkyl phosphonates is to gain a better understanding of the reaction that converts carbon–chlorine bonds in chlorofluorocarbons into carbon–hydrogen bonds. We have found that the Atherton–Todd reaction is one of the few such reactions that can be used to effect this interconversion. The experimentally found order of reactivity to dialkyl phosphonates follows the sequence: $CCl_4 > CCl_4F > CCl_2F_2$, and no reaction is observed at a carbon atom that also contains a carbon–hydrogen bond.[13] This relative reactivity order of chlorofluorocarbons to dialkyl phosphonates is difficult to understand. We have therefore also carried out calculations on chlorofluoromethanes in order to ascertain whether we can better understand these reactivity patterns of chloro- and fluoro-substituted methanes with dialkyl phosphonates. Although extensive calculations on chlorofluoromethanes by the application of different basis sets have been recently reported, none of these calculations have incorporated a correction for correlation effects.[14] We have therefore carried out calculations which include such a correction, and in this paper we use the results of these calculations on both chlorofluoromethanes and dialkyl phosphonates to develop a better understanding of the Atherton–Todd reaction as it relates to substituted chlorofluoroalkanes.

Computational Methodology

Calculations were carried out on an IBM RISC System/6000 workstations using the GAUSSIAN 90 quantum mechanical package, developed by Pople and co-workers.[15] Reaction coordinates were calculated with the standard 3-21G(*) basis set.[16] All structures were fully optimized applying a basis set that is designated further in the text as 6-31+G*. It was constructed from the underlying 6-31G*[17] representation by the addition of a single set of diffuse Gaussian s- and p-functions,[18] for which it has been shown to improve significantly the description of anionic systems.[19] We applied the same basis set also toward neutral systems in order to have an adequate basis for energy comparison. When appropriate, the existence of different conformers was investigated, and the most stable of them were further used for calculation of activation and reaction energies as well as for relative basicities and acidities. Transition structures were computed using the eigenvector following procedure which is included as part of the GAUSSIAN 90 package.[20] The curvature of the potential energy surface in all of its located critical points was confirmed with analytical second derivatives. Frozen-core Møller–Plesset (MP2) perturbation theory was applied to correct for correlation effects.[21] Corrections for zero-point vibrational energy have been estimated from the 6-31+G* harmonic frequencies (scaled by 0.9).[22]

Models

Dimethyl phosphonate (**1**) and dimethyl chlorophosphate (**2**) as well as a series of chlorofluoromethanes and their corresponding hydrogen derivatives (Table II), were selected as representative

(7) See, for example: Troev, K.; Roundhill, D. M. *Phosphorus and Sulfur* **1988**, *73*, 189–95 and references therein.
(8) Troev, K.; Kirilov, E. M. G.; Roundhill, D. M. *Bull. Chem. Soc. Jpn.* **1990**, *63*, 1284–5.
(9) (a) Abramov, B. *Proc. Acad. Sci. USSR, Chemistry Sect.* **1950**, *73*, 487. (b) Yurchenko, R. L.; Yurchenko, V. G.; Podgornyi, A. V. *Zh. Obshch. Khim.* **1991**, *61*, 772–4.
(10) (a) Pudovik, A. *Thesis from the Proceedings of the General Assembly of Academy of Science USSR, Chemistry Section*, October, 1947. (b) Cherkasov, R. A.; Galkin, V. I.; Khabibullina, A. B.; Al Kurdi, K. *Phosphorus, Sulfur, Silicon and Related Elements* **1990**, *49/50*, 61–4.
(11) Van Wazer, J. R.; Ewig, C. S. *J. Am. Chem. Soc.* **1986**, *108*, 4354–60.
(12) Ewig, C. S.; Van Wazer, J. R. *J. Am. Chem. Soc.* **1985**, *107*, 1965–71.
(13) Georgiev, E. M.; Roundhill, D. M.; Troev, K. *Inorg. Chem.* **1992**, *31*, 1965–8.
(14) Cooper, D. L.; Wright, S. C.; Allan, N. L.; Winterton, N. S. *J. Fluorin. Chem.* **1990**, *47*, 489–507.
(15) GAUSSIAN 90. Revision I, Frisch, M. J.; Head-Gordon, M.; Trucks, G. W.; Foresman, J. B.; Schlegel, H. B.; Raghavachari, K.; Robb, M.; Binkley, J. S.; Gonzalez, C.; DeFrees, D. J.; Fox, D. J.; Whiteside, R. A.; Seeger, R.; Melius, C. F.; Baker, J.; Martin, R. L.; Khan, L. R.; Stewart, J. J. P.; Topiol, S.; Pople, J. A. Gaussian Inc., Pittsburgh, PA, 1990.
(16) (a) Binkley, J. S.; Pople, J. A.; Hehre, W. J. *J. Am. Chem. Soc.* **1980**, *102*, 939. (b) Gordon, M. S.; Binkley, J. S.; Pople, J. A.; Pietro, W. J.; Hehre, W. J. *J. Am. Chem. Soc.* **1982**, *104*, 2797. (c) Pietro, W. J.; Francl, M. M.; Hehre, W. J.; DeFrees, D. J.; Pople, J. A.; Binkley, J. S. *Am. Chem. Soc.* **1982**, *104*, 5039.
(17) (a) Hehre, W. J.; Ditchfield, R.; Pople, J. A. *J. Chem. Phys.* **1972**, *56*, 2257. (b) Hariharan, P. C.; Pople, J. A. *Theor. Chim. Acta* **1973**, *28*, 213. (c) Binkley, J. S.; Gordon, M. S.; DeFrees, D. J.; Pople, J. A. *J. Chem. Phys.* **1982**, *77*, 3654. (d) Hehre, W. J.; Radom, L.; Schleyer, P. v. R.; Pople, J. A. *Ab initio Molecular Orbital Theory*; Wiley: New York, 1986; Section 4.3.
(18) (a) Clark, T.; Chandrasekhar, J.; Spitznagel, G. W.; Schleyer, P. v. R. *J. Comput. Chem.* **1983**, *4*, 294. (b) Spitznagel, G. W.; Clark, T.; Chandrasekhar, J.; Schleyer, P. v. R. *J. Comput. Chem.* **1982**, *3*, 363.
(19) For full discussion of the basis set, see: Hehre, W. J.; Radom, L.; Schleyer, P. v. R.; Pople, J. A. *Ab Initio Molecular Orbital Theory*; Wiley: New York, 1986; pp 86–88 and references therein.
(20) Gonzalez, C.; Schlegel, H. B. *J. Chem. Phys.* **1989**, *90*, 2154–61.
(21) DeFrees, D. J.; Levi, B. A.; Pollack, S. K.; Hehre, W. J.; Binkley, J. S.; Pople, J. A. *J. Am. Chem. Soc.* **1979**, *101*, 4085–9.
(22) Pople, J. A.; Schlegel, H. B.; Krishnan, R.; DeFrees, D. J.; Binkley, J. S.; Frish, M. J.; Whiteside, R. A.; Hout, R. A.; Hehre, W. J. *Int. J. Quantum Chem. Symp.* **1981**, *15*, 269–78.

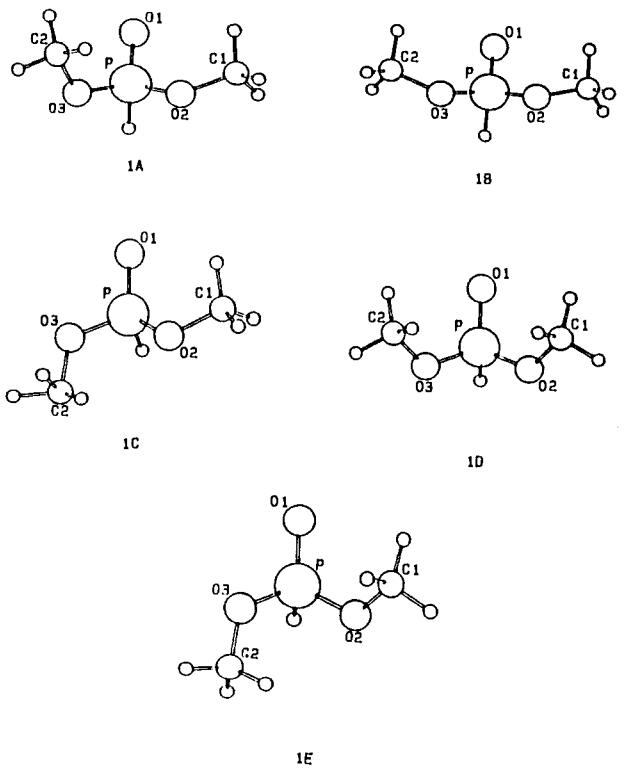

Figure 1. HF/6-31+G* predicted geometries for the dimethyl phosphonate. **1A** is the global minimum and **1D** is a transition structure.

compounds for carrying out the computational study of the reaction shown in eq 1. In addition to these compounds, a number of monomethyl- and dimethyl-substituted derivatives of phosphonic and phosphorous acids were also computed (Table I). The latter compounds are discussed further in the text as plausible intermediates in the reaction. Further simplification of the chosen systems was required, however, in order to calculate adducts and transition structures that have an exceptionally large number of variables and/or basis function. Among the simplifications that were made was the substitution of the methyl groups with hydrogen. Thus phosphonic acid and its anion as well as the anion of phosphorous acid were the simplest phosphorus-containing models used. Ammonia was selected as a model base for the computational study of the basic activation in the Atherton–Todd reaction. The ammonium cation, as well as methylammonium cation, which are possible intermediates in two concurrent model reactions, were also considered, and their corresponding calculated energies are listed in Table II.

Results

Dimethyl Phosphonate (1) and Dimethyl Chlorophosphate (2). Five critical points were located on the potential energy surface of dimethyl phosphonate in a 6-31+G* basis. These structures **1A–E** are shown in Figure 1. With the exception of **1D**, all other structures correspond to energy minima, i.e., to stable conformers. These conformers result from rotations about the C–O bonds in the molecule. In two of them, **1A** and **1B**, the methyl groups are roughly adjacent to the phosphoryl oxygen and slightly rotated away from the corresponding O—P=O planes, whereas in **1C** and **1E** one of the methyl group is opposed to the phosphoryl oxygen. The stationary point **1D** corresponds, according to our calculations, to a transition structure with a single imaginary frequency at 27 i cm^{-1} due to a delocalized motion of both methoxy groups. Ewig and Van Wazer found three conformers for dimethyl phosphonate based on STO-3G* conformational analysis.[11] The conformers they reported correspond to the structures **1A–C** on Figure 1. In a more recent spectroscopic study of the molecule of dimethyl phosphonate, five possible conformers of the type **1A–E** were considered based on molecular mechanics calculations.[23] According to the computed energies of the different conformers summarized in Table I, **1A** is the global minimum structure. This result is in agreement with that predicted by Ewig and Van Wazer based on 4-31G*//STO-3G* calculations.[11] The main differences in the geometry of dimethyl phosphonate when optimized using a 6-31+G* basis set as compared to the previous published data is a slightly longer P=O double bond (ca. 0.015 Å), along with shorter P–O and P–H bonds, and larger values for the C–O–P angles.[11]

The three stable conformers for dimethyl chlorophosphate **2A–C** correspond to the same type as the dimethyl phosphonate conformers **1A–C**, but their predicted order of relative energies is different. Thus conformer **2C** is predicted to be the global minimum for dimethyl chlorophosphate with one methyl group roughly adjacent to the phosphoryl oxygen and the other to the chlorine atom.

No significant geometrical changes occur in other parts of the molecule when the hydrogen from the P–H bond in dimethyl phosphonate (**1**) is substituted by chlorine in dimethyl chlorophosphate (**2**). There is, however, a slight shortening of the P=O and P–O bond lengths, which is consistent with the results of Gordon and Schmidt, who found that electronegative substituents at phosphorus lead to a shortening of the P–O bond.[24]

Monomethyl Phosphonate (3) an Its Anion (4). Four energy minimum structures **3A–D** were found for the monomethyl phosphonate in the 6-31+G* basis, resulting in four conformers (Figure 2). The conformations **3A** and **3B** of the monoester have their methyl groups and the hydrogen of the hydroxy group roughly adjacent to the phosphoryl oxygen and rotated slightly away from it in the same direction. This direction is clockwise for the conformer **3B** when looking at the phosphoryl oxygen down the P=O double bond and anticlockwise for **3A**. The other two conformers **3C** and **3D** have the methyl group and, respectively, the hydrogen of the hydroxy group opposed to the phosphoryl oxygen, while the other group is adjacent to it. The conformer **3B** is calculated to be the global minimum structure of this molecule.

For the anion of the monomethyl phosphonate we have computed three stable conformers **4A–C**, which are shown in Figure 3. Their relative energies are within the range of 0.6 kcal/mol, and two of them, **4A** and **4C**, are predicted to have energy differences of less than 0.1 kcal/mol. The different conformer type found here is essentially the same as those found for the monomethyl phosphonate. These conformers arise from the three possible orientations of the methyl group. This methyl group is opposed to the O^1 oxygen to which it is not directly connected as in **4A** or rotated slightly away from the O^2–P–O^1 plane in the two possible directions as computed for **4B** and **4C**. Not surprisingly, the charge delocalization in this anion results in practically equal bond lengths (av 1.482 Å in the three conformers **4A–C**) between the phosphorus atom and the O^1 and O^3 oxygens not connected to a methyl group. These bond distances have values closer to that of the P=O double bond (av 1.452 Å in **3A–D**) than that of the P–OH single bond (av 1.589 Å), as computed in the four conformers of the monomethyl phosphonate.

Phosphonic Acid (5) and Its Anion (6). We have located two stationary points (**5A** and **5B**) on the potential energy surface of the phosphonic acid using the 6-31+G* basis set. They have an energy difference of less than 0.1 kcal/mol, as is evident from the data collected in Table I, and their geometrical parameters differ only slightly with respect to both of the H—O—P=O dihedral angles. The structure **5A** adopts C_s symmetry, which is similar to the only conformation of this compound that was computed by Ewig and Van Wazer.[12] A frequency analysis of this particular

(23) Monahova, N. I.; Katzuba, S. A.; Ashrafulina, L. H.; Shagidulin, R. R. *J. Prikl. Spektrosk.* **1989**, *49*, 944–50.
(24) Schmidt, M. W.; Gordon, M. S. *J. Am. Chem. Soc.* **1985**, *107*, 1922–30.

Table I. Energies of the Phosphorus-Containing Structures[a]

	compound	conformer[b]	6-31+G*//6-31+G*	MP2/6-31+G*//6-31+G*	ZPE[c]	RE[d]	n^e
1		A	−645.17830	−646.09095	61.5	0.0	0
		B	−645.17575	−646.08742	61.2	1.9	0
		C	−645.17464	−646.08756	61.4	2.0	0
		D	−645.17750	−646.08980	61.3	0.5	1
		E	−645.17516	−646.08824	61.4	1.6	0
2		A	−1104.10811	−1105.15413	56.5	0.4	0
		B	−1104.10831	−1105.15455	56.6	0.2	0
		C	−1104.10796	−1105.15502	56.7	0.0	0
3		A	−606.15234	−606.93660	43.9	1.2	0
		B	−606.15432	−606.93876	44.1	0.0	0
		C	−606.15045	−606.93505	43.9	2.1	0
		D	−606.14971	−606.93436	44.0	2.7	0
4	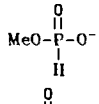	A	−605.61158	−606.41357	36.7	0.0	0
		B	−605.61101	−606.41264	36.7	0.6	0
		C	−605.61158	−606.41356	36.7	0.0	0
5		A	−567.12805	−567.78408	26.3	0.0	1
		B	−567.12805	−567.78419	26.4	0.0	0
6		A	−566.59029	−567.26359	19.6	0.0	0
		B	−566.59029	−567.26361	19.6	0.0	0
7	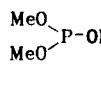	A	−645.16038	−646.07370	61.0	2.4	0
		B	−645.16255	−646.07752	61.0	0.0	0
		C	−645.16105	−646.07538	61.0	1.3	0
		D	−645.16072	−646.07542	60.8	1.1	0
8	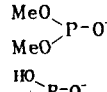	A	−644.59753	−645.53435	53.2	0.0	0
		B	−644.59763	−645.53436	53.4	0.1	0
		C	−644.59746	−645.53452	53.4	0.1	0
9		A	−566.55670	−567.23505	19.2	0.0	0
		B	−566.55211	−567.23103	19.2	2.5	0
10		A	−605.57584	−606.38350	36.3	1.4	0
		B	−605.57593	−606.38352	36.3	1.4	0
		C	−605.57847	−606.38596	36.4	0.0	0
	TS1		−701.30282	−702.40186	84.0		1
	ADD 1		−701.37696	−702.48009	86.0		0
	TS2		−645.04086	−645.98666	58.3		1
	TS3		−605.47593	−606.31211	33.8		1
	TS4		−1133.71078	−1135.05916	44.4		1

[a] Energies in hartrees. [b] Structures optimized using HF/6-31+G* basis set. [c] Zero-point vibrational energies in kcal/mol, scaled by 0.9. [d] Relative energies between the conformers calculated on MP2/6-31+G*//6-31+G* + ZPE level. [e] Number of imaginary frequencies.

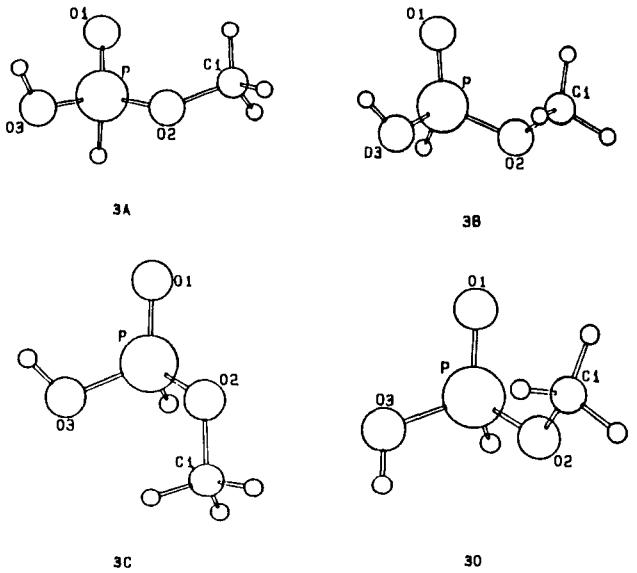

Figure 2. HF/6-31+G* predicted geometries for the stable conformers of monomethyl phosphonate 3. The global minimum structure is 3B.

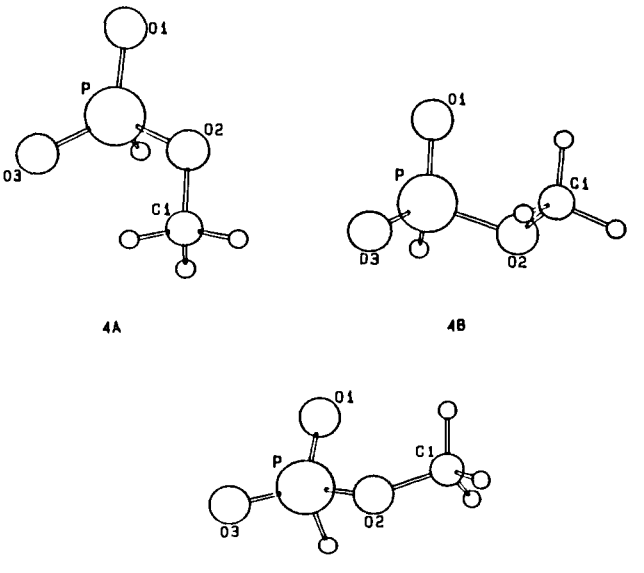

Figure 3. HF/6-31+G* predicted geometries for the stable conformers of monomethyl phosphonate anion 4.

structure indicates the presence of a single imaginary frequency at 46 i cm^{-1}, which corresponds mainly to the O–H vibrations in both of the hydroxyl groups. This result implies that **5A** is a transition structure. In the true minimum structure **5B**, the dihedral angles between the H—O—P and the O—P=O planes are 0.4 and −24.4°, respectively. In this geometry one of the hydrogens lies essentially in the O—P=O plane, and the other one is rotated −24.4° away from the other corresponding O—P=O plane.

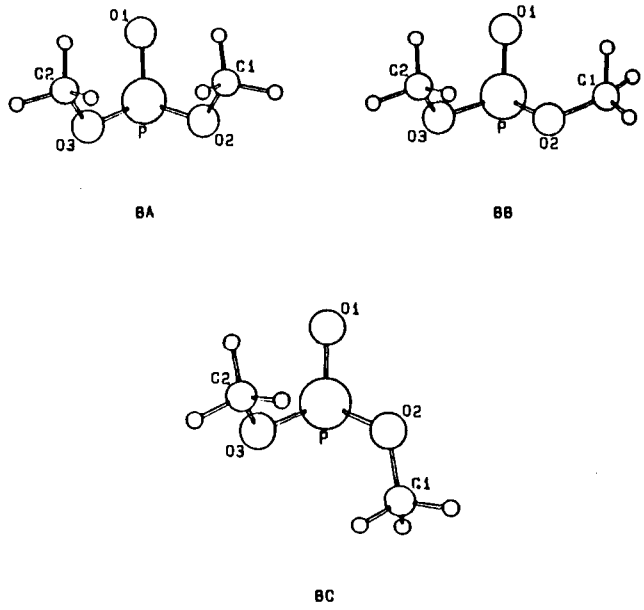

Figure 4. HF/6-31+G* optimized geometries for the stable conformers of the dimethyl phosphite anion. Conformer **8A** is the lowest energy structure.

Two energy minimum structures have been computed for the anion of the phosphonic acid and designated as conformers **6A** and **6B** in Table I. Again, by analogy with the structures of the anion of monomethyl phosphonate, **4A–C**, the bond lengths between the phosphorus atom and the two oxygens not connected to a hydrogen atom have the same value in both conformers **6A** and **6B** (av 1.483 Å). The value is closer to that of the phosphoryl bond length in **5B** (1.456 Å), and the effect is due to the charge delocalization.

Dimethyl Phosphite (7) and Its Anion (8). The conformational analysis of dimethyl phosphite results in there being the four energy minimum structures **7A–D**. Conformer **7B** is the global minimum structure among the four conformers, as is apparent from the data for these conformers listed in Table I.

For the dimethyl phosphite anion **8**, the theoretical number of conformers is less than that of the corresponding neutral phosphite **7**. Consequently only three stable conformers **8A–C** have been located on 6-31+G* level for that compound (Figure 4). The three conformers **8A–C** are of the same type as those found for dimethyl phosphite **7**, with the exception that there is only one conformer **8B** that has its methyl groups opposed to the O^1 oxygen atom. An interesting structural feature of the anion **8** is the significant shortening of the P–O bond (av 1.503 Å) as compared to its average length of 1.628 Å in the P–OH structural fragment of dimethyl phosphite **7**. This average value of the P–O bond in **8** is closer to that of a phosphoryl bond, which implies that it has partial double character. In terms of the resonance formalism, this means that there is a significant contribution from the first resonance structure that is shown in the representation in eq 3.

$$(MeO)_2P^-{=}O \leftrightarrow (MeO)_2P{-}O^- \qquad (3)$$

This conclusion is also supported by comparison of the total atomic charges for the most stable conformers of dimethyl phosphite **7** and its anion **8**. These data are given in Table III. This comparison indicates that there is a larger increase in the negative charge on the phosphorus atom (from 1.42 in **7B** to 1.11 in **8A**) as compared to that on the O^1 oxygen atom (from −1.00 to −1.10 in **7B** and **8A**, respectively) from which the proton has been removed in **8A**. At the same time, the charges on the oxygen atoms of the methoxy groups decrease slightly as is shown by the data listed in the Table III.

Table II. Energies[a] of some Chlorofluoro-Substituted Methanes and Nitrogen-Containing Species Used as Model Compounds in the Computational Study of the Atherton–Todd Reaction

structure	symmetry	6-31+G* HF	6-31+G* MP2	HF/6-31+G* zero pt[c]
CCl_4	T_d	−1875.74720	−1876.46683[b]	6.1
$CFCl_3$	C_{3v}	−1515.71957	−1516.47086[b]	7.1
CF_2Cl_2	C_{2v}	−1155.69613	−1156.47747[b]	8.3
$CHCl_3$	C_{3v}	−1416.87194	−1417.43972[b]	12.4
$CHFCl_2$	C_1	−1056.83774	−1057.43918[b]	13.5
CHF_2Cl	C_1	−696.80924	−697.44292[b]	14.6
CCl_3^-	C_{3v}	−1416.28150	−1416.85118[b]	3.2
$CFCl_2^-$	C_s	−1056.24299	−1056.84785[b]	3.8
CF_2Cl^-	C_s	−696.20308[d]	−696.87420[b]	4.4[e]
NH_3	C_{3v}	−56.18950	−56.36265	20.9
NH_4^+	T_d	−56.53128	−56.70041	30.0
$CH_3NH_3^+$	C_1	−95.57416	−95.86916	48.1

[a] Energies in hartrees. [b] Structures optimized using MP2/6-31+G*//MP2/6-31+G* basis set. [c] Zero-point vibrational energies in kcal/mol scaled by 0.9. [d] Estimated on MP2/6-31+G* optimized geometry since this anion does not have energy minimum on SCF level and optimizes to CCl_2 and Cl^- instead. [e] Obtained by numerical frequency evaluation with MP2/6-31+G* basis set.

Table III. Total Atomic Charges on the Heavy Atoms of the Most Stable Conformers of Dimethyl Phosphite (7) and Rs Anion (8) from Mulliken Population Analysis on HF/6-341+G* Basis $(C^3H_3O^3)(C^3H_3O^2)POH$

atom	7B	8A	atom	7B	8A
P	1.42	1.11	O^3	−0.85	−0.66
O^1	−1.00	−1.10	C^2	−0.34	−0.31
O^2	−0.78	−0.66	C^3	−0.35	−0.31

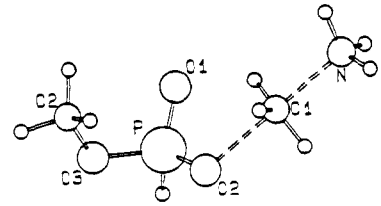

Figure 5. HF/6-31+G* optimized geometry of the transition structure for the dealkylation of dimethyl phosphonate **1** by ammonia TS1:O2–C1 = 2.083 Å; C1–N = 1.936 Å.

Anions of Phosphorus Acid (9) and Its Monomethyl Ester (10). Conformational analysis for these two compounds results in the identification of three stable conformers for the anion of the monoester **10A–C** and two conformers for the anion of phosphorus acid, **9A** and **9B**. By analogy to the structure of **5A** that was computed for phosphonic acid, the conformer of the phosphorous acid anion **9A** adopts C_s symmetry. This conformer **9A** is a true minimum, unlike **5A** which is a transition structure. In both the anion of phosphorous acid **9** and its monomethyl ester **10**, the P–O bond length between phosphorus and the oxygen atom which has three lone pairs of electrons associated with it, is shorter than the other P–O bonds. The shortening of the bond length in these molecules is due to the same reasons as was discussed for the dimethyl phosphite anion **8**.

Transition Structure for the Dealkylation of Dimethyl Phosphonate by Ammonia (TS1). The transition structure for this reaction (Figure 5) represents a typical S_N2 displacement at the aliphatic carbon atom. The three atoms O–C–N lie almost on a straight line with the bond distances O–C and C–N being 2.083 and 1.936 Å, respectively. The elongated O–C bond distance, along with the relatively small values of the HCO bond angles (av 85.2°), are characteristic of a late transition structure that can be expected for an endothermic process. The normal mode of the single imaginary frequency at 586 i cm^{-1} that is present in the calculated vibrational spectrum of TS1 is mainly due to the O–C stretch.

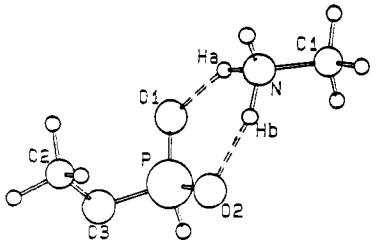

Figure 6. HF/6-31+G* predicted geometry for the ion pair adduct between the anion of monomethyl phosphonate **4** and methylammonium cation: O1–Ha = O2–Hb = 1.740 Å.

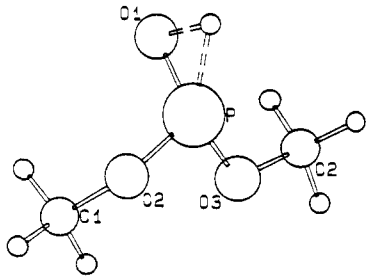

Figure 7. HF/6-31+G* optimized geometry of the transition structure TS2 for the noncatalyzed isomerization of dimethyl phosphonate **1** to dimethyl phosphite **7**.

Ion Pair Adduct between the Anion of Monomethyl Phosphonate and Methylammonium Cation (ADD1). A computational search on the HF/6-31+G* level for critical points on the potential energy surface of a system containing these two cations results in the location of the energy minimum structure ADD1, shown in Figure 6. According to the calculations the methylammonium cation forms two weak hydrogen bonds with the phosphonate anion, where two of the amine hydrogens Ha and Hb are coordinated to the two oxygen atoms O1 and O2, respectively. The six-membered ring that is formed consists of the two hydrogen-bonded O–P–O and H–N–H fragments (Figure 6). It is essentially planar with esentially equal interatomic distances of a given type: P–O = 1.501; O–H = 1.740 and N–H = 1.035 Å, respectively.

Transition Structures of the Noncatalyzed Tautomerization of Monomethyl Phosphonate Anion to Monomethyl Phosphite Anion (TS3) and of Dimethyl Phosphonate to Dimethyl Phosphite (TS2). The three-centered transiton states TS2 (Figure 7) and TS3 reveal, after analysis of the analytical second derivative matrix, in each case a single imaginary frequency at 2180 and 2187 *i* cm^{-1}, respectively. These normal modes correspond mainly to the P–H vibration. In both transition structures, the P–H, P–O (phosphoryl), and the O–H (to be formed) bond lengths have intermediate values as compared to those for the different conformers.

Transition Structure of the Proton Transfer Reaction between Phosphonic Acid and Its Anion (TS4). This transition structure of the model deprotonation reaction was located on the 6-31+G* level. Its single imaginary frequency, 1521 *i* cm^{-1} corresponds mainly to the P–H stretch (Figure 8). The three atoms (P, H, and O) involved in the proton-transfer step lie on an almost straight line (∠PHO = 176.0°). The proton transfer is in the middle of the transition with the P–H bond partially broken 1.674 Å (1.374 Å in phosphonic acid **8**) and the O–H bond partially formed 1.229 Å (0.951 Å in phosphonic acid). The phosphoryl bond length also has an intermediate value of 1.486 Å as compared to the regular distances found in the phosphonic acid (1.456 Å) and the phosphite anion (1.515 Å) **10**.

Discussion

Possible Pathways of Basic Activation of Dimethyl Phosphonate with Ammonia. We discuss here two possible reactions that can occur between dimethyl phosphonate and ammonia. These reactions are (i) deprotonation of the phosphonate at phosphorus

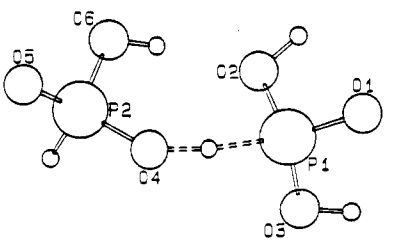

Figure 8. HF/6-31+G* optimized geometry for the transition structure of the model P–H deprotonation of phosphonic acid by its anion TS4.

$$(CH_3O)_2P(O)H + NH_3 \rightleftharpoons [(CH_3O)_2PO]^- + NH_4^+ \quad (4)$$

and (ii) dealkylation of the alkoxy group

$$(CH_3O)_2P(O)H + NH_3 \rightleftharpoons [(CH_3O)PHOO]^- + CH_3NH_3^+ \quad (5)$$

Another possibility is that of amine attack at the phosphorus center to form a pentacoordinated phosphorane intermediate. This latter reaction, because of its nature, is not related to Atheton–Todd chemistry and is the subject of a parallel theoretical study.[25] From our data in Tables I and II, the overall reaction energies estimated on the MP2 + ZPE level for the reactions according to eqs 4 and 5 are 209.7 and 109.2 kcal/mol, respectively. These values show that both processes are endothermic and therefore thermodynamically unfavorable in the gas phase. The nature of these two reactions (eqs 4 and 5), which in each case yield a pair of ionic species from two neutral molecules, emphasizes the important role that solvation effects and hydrogen bonding play in the stabilization of the final products in solution. An important result supporting this suggestion is the calculated hydrogen-bonded ion pair ADD1 (Figure 6) between the products of the dealkylation reaction 5. Its total energy is in fact 13.0 kcal/mol lower than that of the reactants (dimethyl phosphonate and ammonia), so that the gas-phase reaction leading to its formation is actually exothermic. This ion adduct ADD1 is in good approximation with an autosolvation model for reaction 5, which clearly indicates that the reaction energy for this process is substantially lower in solution than calculated for the gas phase. In a previous experimental study of the dealkylation reaction in a two-component system containing dimethyl phosphonate and an amine, it was found that the following order of increasing reactivity was followed for the different types of amines: $H_2NR > HNR_2 > R_3N$.[26] This finding supports the above suggestion about the role of the hydrogen bonding in the dealkylation reaction since the order correlates with the number of hydrogens on the amine rather than with the relative base strength.

The most important reason for us to reject the direct deprotonation pathway (**4**) is the fact that the reaction coordinate search along the N—H–P distance, employing the 3-216(+) basis set, does not indicate the presence of a stationary point along this reaction coordinate. This N—H–P distance was searched from 2.5 to 1.1 Å employing 0.2 Å steps. Attempts to locate transition structures on a 3-21G(*) level when this distance was allowed to vary independently at two points 1.5 and 1.2 Å resulted in the effective separation of the two molecules. In contrast to this computational result, the dealkylation pathway search resulted in the location of a critical point TS1 corresponding to a late transition structure in the S_N2 substitution at the carbon atom (Figure 5) as well as of the ion pair adduct ADD1 between the

(25) Kaneti, J.; Georgiev, E. M.; Troev, K.; Roundhill, D. M., paper in preparation.
(26) Troev, K.; Georgiev, E. M., unpublished data.

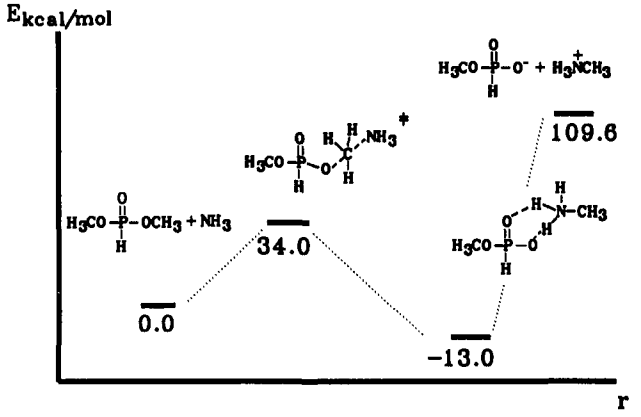

Figure 9. MP2/6-31+G*//HF/6-31+G* energy profile of the gas-phase dealkylation reaction of dimethylphosphonate 1 by ammonia.

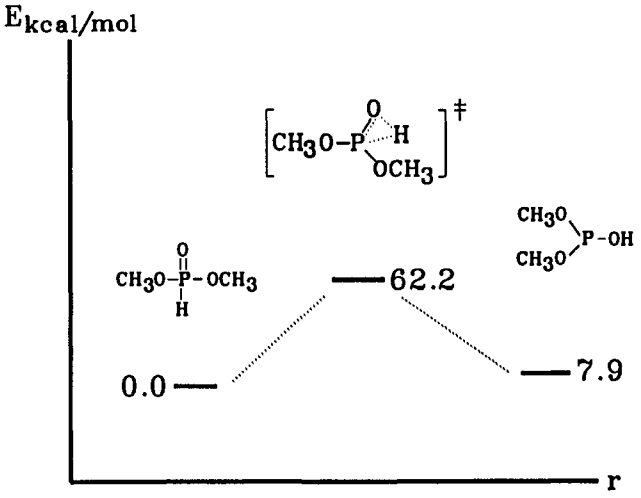

Figure 10. MP2/6-31+G*//HF/6-31+G* energy profile of the gas-phase noncatalyzed isomerization of dimethyl phosphonate 1 to dimethyl phosphite 7.

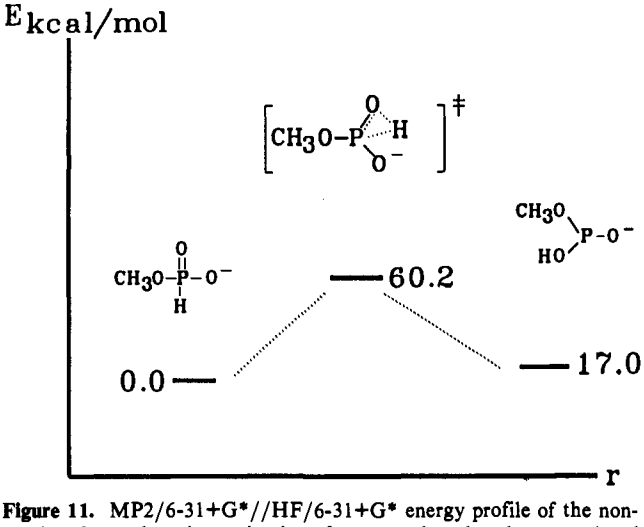

Figure 11. MP2/6-31+G*//HF/6-31+G* energy profile of the non-catalyzed gas-phase isomerization of monomethyl phosphonate anion 4 to the anion of monomethyl phosphite 8.

anion of monomethyl phosphonate 4 and methylammonium cation (Figure 6). The energy profile of this gas-phase reaction is presented in Figure 9. The calculated activation energy for this reaction (eq 5), on a MP2 + ZPE level using the data in Tables I and II, is 34.0 kcal/mol, which is 75.6 kcal/mol lower than the energy of the separated products.

The high-energy difference between the dealkylation and the deprotonation pathways (100.5 kcal/mol) in favor of the dealkylation as calculated on the MP2 + ZPE level for the overall reactions in eqs 4 and 5 further indicates that the direct deprotonation of dimethyl phosphonate by ammonia is rather unlikely. The conclusion is also supported from the calculated relative proton affinities (Table V) and acidities (Table VI) that have been computed for some of the acids and bases that can be used for the Atherton–Todd reaction. These values have been calculated using the data in Tables I and II. Ammonia is calculated to be the weakest base among those collected in Table V. The anion of dimethyl phosphonate, $[(CH_3O)_2PO]^-$ (**8**), is the strongest phosphorus-containing base. The anion of monomethyl phosphonate, $[(CH_3O)PHOO]^-$ (**4**), is a relatively weak base that is stabilized by charge delocalization.

Phosphonate–Phosphite Noncatalyzed Tautomerization of Dimethyl Phosphonate and of the Anion of Monomethyl Phosphonate. Another argument that has been presented in order to explain the deprotonation of dialkyl phosphonates by amines is that the dialkyl phosphonates first tautomerize to their more acidic phosphite form.

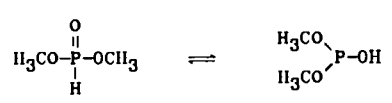

(6)

1 7

In order to evaluate whether such a tautomerization is a realistically possible step in the Atherton–Todd reaction, we have calculated the transition structure TS2 for such noncatalyzed reaction (Figure 7). In addition, we have also computed the tautomerization of the monomethyl phosphonate anion **4** to its three coordinated phosphite form **10**.

Table IV. Main Components of the Transition Vector in Å and deg for the Phosphonate–Phosphite Tautomerization Transition Structures TS2 and TS3

structure[a]	P–H	P–O	O–H	<PHO
TS2	1.485	1.573	1.335	51.3
TS3	1.488	1.534	1.384	54.5

[a] Optimized with HF/6-31+G* basis set.

Table V. Calculated Relative Proton Affinities of Some of the Bases Listed in Tables I and II

	$\delta\Delta E^a$		
base, B	SCF	MP2	MP2 + ZPE
NH_3	−150.0	−201.1	−209.7
$[HOP(O)(H)O]^-$ (6)	−26.9	−22.6	−21.0
$[CH_3OP(O)(H)O]^-$ (4)	−23.8	−19.7	−18.8
$[HOP(O)OH]^-$ (9)[b]	−5.8	−4.7	−3.4
$[CH_3OP(O)OH]^-$ (10)[b]	−3.1	−2.4	−1.8
$[(CH_3O)_2PO]^-$ (8)[b]	0.0	0.0	0.0
CCl_3^-	6.1	20.0	19.1
$CFCl_2^-$	8.8	21.8	20.4
CF_2Cl^-	15.9	24.5	22.6

[a] Energies in kcal/mol for the reaction $BH^+ + [(CH_3O)_2PO]^- \rightarrow B + (CH_3O)_2P(O)H$. [b] The BH^+ molecule contains a P–H bond.

Table VI. Calculated Relative Acidities of the Phosphorus Acids Listed in Table I

	$\delta\Delta E^a$		
acid, A	SCF	MP2	MP2 + ZPE
$(CH_3O)_2P(O)H$ (1)	0.0	0.0	0.0
$(HO)_2P(O)H$[b] (5)	5.9	4.7	3.6
$(CH_3O)_2POH$ (7)	9.9	8.5	8.0
$(CH_3O)(OH)P(O)H$ (3)	23.9	19.8	18.9
$(HO)_2P(O)H$[c] (5)	26.9	22.6	21.1

[a] For the reaction $A^- + (CH_3O)_2P(O)H \rightarrow AH + [(CH_3O)_2PO]^-$. [b] P–H acidity. [c] O–H acidity.

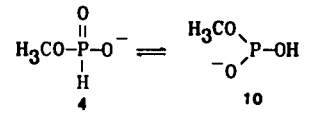
(7)

4 10

The principal reason for making this calculation is that recently, on the basis of experimental evidence, we have proposed that the initial step of the Atherton–Todd involves dealkylation of the dialkyl phosphonate by the base acting as a nucleophile to give the anion $(RO)P(O)H(O)^-$. This anion then reacts with CCl_4 to give the monoalkyl chlorophosphate $(RO)P(O)Cl(OH)$ and the trichloromethanide anion CCl_3^- (Scheme II).[13] In order to rationalize the formation of a P–Cl bond by this dealkylation pathway we have invoked a subsequent tautomerization step whereby the tetracoordinated intermediate $(RO)P(O)H(O)^-$, which has the negative charge on oxygen, converts to the tricoordinated form $(RO)P(O)OH^-$, which has the negative charge localized primarily on the phosphorus center.

Scheme II

$$(RO)_2P(O)H + NR'_3 \rightarrow (RO)P(O)H(O)^- + NRR'_3{}^+$$

$$(RO)P(O)H(O)^- \rightarrow (RO)P(O)OH^-$$

$$(RO)P(O)OH^- + CCl_4 \rightarrow (RO)P(O)Cl(OH) + CCl_3^-$$

In order to check whether this suggestion can be supported on theoretical grounds, we have computed the structures of all of the species, including the transition structure TS3 that can be involved in the noncatalyzed tautomerization of the monomethyl phosphonate anion (eq 7).

Although there is no direct experimental evidence for the existence of the two three-coordinated phosphorus species **7** and **10** in the above reactions, the tautomerization of dialkyl phosphonates to dialkyl phosphites has been often invoked in order to explain the mechanism of other reactions of dialkyl phosphonates that result in P–H bond cleavage.[6] The energy profiles of these two reactions are presented in Figures 10 and 11. The tautomerization energy of 7.9 kcal/mol for dimethyl phosphonate has a value that is close to that of 9.8(2.6) kcal/mol reported by Guthrie for the isomerization of diethyl phosphonate. This value of 9.8 kcal/mol was calculated from thermodynamic data for an aqueous solution at 25 °C, which may explain the difference in the two calculated values.[28] This result suggests that the species **1** and **7** involved in this tautomerization have similar solvation energies, thereby maintaining the same energy difference in both the gas state and in solution. Although the activation energy for the noncatalyzed tautomerization of the monomethyl phosphonate ion is calculated to be lower by 1.7 kcal/mol on the MP2 + ZPE level than that for the dimethyl phosphonate, as we have initially suggested, it still remains significantly high in absolute values in order for the noncatalyzed process (eqs 6 and 7) to be likely to occur. These computational results provide indirect support for the early considerations of Hammond that the tautomerization of dialkyl phosphonates is a catalytic process which is accelerated by the presence of bases and acids.[27]

The Role of the Phosphonate Anion in the Promotion of the Atherton–Todd Reaction. Consideration of these theoretical results leads one to the conclusion that a direct tautomerization step that converts a four-coordinated phosphonate into a three-coordinated phosphite intermediate is rather unlikely. Our calculations as well as the experimental results[2-5] indicate that amines are alkylated and not protonated by dialkyl phosphonates. This alkylation reaction leads to the formation of another basic species, the anion of monoalkyl phosphonate (eq 5), which is the conjugate base of the starting amine. A reasonable assumption based on these facts is the possibility that the monoalkyl phosphonate anion that is obtained is the actual base which is capable of deprotonating the dialkyl phosphonate to generate the catalytically active dimethyl phosphite anion (eq 8). This

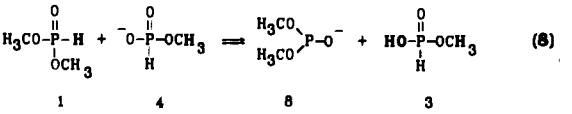
(8)

1 4 8 3

assumption is partially supported by the calculated relative proton affinities for the protonation of the dimethyl phosphonate anion (Table VI). These data indicate that the anion of monomethyl phosphonate (**4**) is much more stronger base than ammonia in this process, although it is still a weaker base than the anion of dimethyl phosphite (**8**). A useful consideration in respect of the possible solvent effects on the equilibrium depicted in eq 8 is the fact that the reaction product and especially monoalkyl phosphonate will be better stabilized by hydrogen bonding with the phosphoryl group-containing species, since in general the Atherton–Todd reaction is carried out in aprotic media[3] and large concentrations of dialkyl phosphonate. The later is converted to dialkyl chlorophosphate, which is also a phosphoryl group-containing molecule. The calculated reaction energy of –18.8 kcal/mol at a MP2 + ZPE level shown in Table V for the reversed reaction indicates only that the equilibrium in eq 8 is shifted toward the reactants in the gas phase. The calculation does not reveal the whole process entirely, since eq 8 does not describe the potential energy surface along the proton-transfer reaction coordinate. In order to locate the transition structure as well as having the ability to search for the anticipated ion–dipole complexes in this system[29] it is necessary to simplify our model compound to accommodate the rising number of variables. Using this simplified model for the compounds shown in eq 9, we have located the transition structure TS4 in this proton-transfer reaction using a 6-31+G* basis set. The calculated total energy of the transition structure, corrected for zero-point vibration (Table I), is –4.7 kcal/mol at a SCF level relative to the reactants in eq 9.

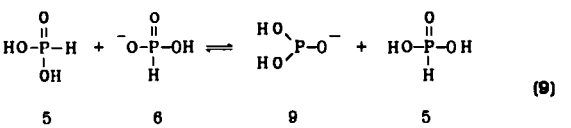
(9)

5 6 9 5

When corrected for correlation effects using MP2/6-31+G*//HF/6-31-G* basis sets, its energy decreases to –7.1 kcal/mol, and –8.6 kcal/mol when the ZPE corrections are included, relative to the separated reactants computed within the same basis. These results demonstrate the significant effect of the MP2 corrections on the energies of transition structures as compared to those of the separated reactants.

We were unable to locate the ion–dipole complexes associated with the reaction shown in eq 9. Analysis of the energies for the early ion–dipole complex searched with a 6-31+G* basis set indicated initially the presence of a relatively flat region in the energy surface which may contain a very shallow minimum. This shallow minimum occurs at an O–H distance of approximately 2.1 Å. Further free optimization of the geometry of this system results, however, in a hydrogen bonded complex between one of the oxygen atoms of the phosphonic acid anion and a hydroxyl group of the phosphonic acid. Similarly the free optimization search at a 6-31+G* level that is downhill from the transition structure for the late ion–dipole complex results in a complex with a hydrogen bond formed between the oxygen atom of the

(27) See, for example: Hammond, P. R. *J. Chem. Soc.* **1962**, 1365–9 and references therein.
(28) Guthrie, J. P. *Can. J. Chem.* **1979**, *57*, 236–9.
(29) Preliminary studies of the potential energy surface along the reaction coordinate for the species involved in eq 8 using a semiempirical (AM1) approach with the MOPAC 6 package revealed, in addition to the proton-transfer transition state, two weakly bonded ion–dipole complexes. The early complex of the pair has an O–H distance of 2.11 Å, and the late complex has a P–H distance of 1.90 Å.

Table VII. Calculated Energies (kcal/mol) of the Reaction between Dimethyl Phosphite Anion (8) and Chloro- and Fluoro-Substituted Methanes: $[(CH_3O)_2PO]^- + CCl_{4-n}F_n \rightarrow (CH_3O)_2P(O)Cl + CCl_{3-n}F_n^-$

n	SCF	MP2	MP2 + ZPE
0	−28.3	−3.2	−2.8
1	−21.5	1.5	1.7
2	−11.1	6.0	5.4

OH group of the phosphonic acid and one of the OH hydrogens in the anion of phosphorous acid. These results imply that the simplified models shown by eq 9 cannot adequately describe the full reaction profile and in particular the ion–dipole complexes of the fully methylated species shown in eq 8. Despite this partial inadequacy in the latter models, the significant result from these calculations is that the energy gained by the system when the early ion–dipole complex is formed is sufficient to overcome the transition structure energy barrier. Since the energy of the transition structure TS4 is lower than that of the separate reactants **5** and **6**, so a significant population of the late ion–dipole complex may be expected. This conclusion is drawn according to the data obtained with the MP2/6-31+G*//HF/6-31+G*+ZPE basis set, which in the present study provides the most reliable basis for energy comparison. Considering the fact that in the late ion–dipole complex the P–H bond should be effectively broken, this means that the catalytically active dialkyl phosphite ion $(RO)_2PO^-$ will be present in form of a weakly bonded complex in these reactions that involve both the diesters of phosphonic acid and the monomethyl phosphonate anion. This pathway can be considered to resemble that originally proposed for the Atherton–Todd reaction. In that originally proposed mechanism, the first step in the reaction involved the removal of a proton from a P–H bond by added base. In our modified mechanism, we now propose that the deprotonation of dimethyl phosphonate occurs by a two-step process, where it is the initially generated monomethyl phosphonate anion that acts as the base toward the P–H bond. From another viewpoint this reaction may be considered as the first step in the base-catalyzed isomerization of dimethyl phosphonate, where the monomethyl phosphonate anion assumes the role of the base.

Interaction between the Dimethyl Phosphite Anion and Chloro- and Fluorosubstituted Methanes. This reaction is actually the second step in the mechanism of the Atherton–Todd reaction according to Scheme I. It is the step that leads to the formation of dimethyl chlorophosphate as one of the final products in the reaction (eq 10).

$$[(CH_3O)_2PO]^- + CCl_{4-n}F_n \rightarrow (CH_3O)_2P(O)Cl + CCl_{3-n}F_n^- \quad (n = 0, 1, 2) \quad (10)$$

As is apparent from the calculated energies of this reaction which are summarized in Table VII, the corrections for the correlation effects have a significant effect on the calculated energies. Thus the reaction of carbon tetrachloride ($n = 0$) with the anion of dimethyl phosphite **8** is calculated to be an exothermic process in the gas phase. At the same time, the reactions with $CFCl_3$ and CF_2Cl_2, for which $n = 1$ and 2, respectively, are computed to be endothermic. This result correlates well with the data of the relative basicities presented in Table V, which indicate increased basicity of the corresponding carbanions $CCl_{3-n}F_n^-$ with increased fluorine content. The data in Table V also show that the anion of dimethyl phosphite **8** is calculated to be weaker base than the above chlorofluorocarbanions. Thus the exothermic character of the reaction of carbon tetrachloride (eq 10; $n = 0$) is a somewhat surprising result and may be explained by the stabilization of the phosphite species when the chlorophosphate product **2** is formed.

Two Possible Alternative Pathways for the Formation of $CHCl_{3-n}F_n$ as One of the Final Products in the Atherton–Todd Reaction. According to Scheme I, the catalytic cycle in the Atherton–Todd reaction is completed with the proton abstraction from dialkyl phosphonate by the carbanion, which in the case of our computational model is expressed in eq 11:

$$(CH_3O)_2P(O)_H + CCl_{3-n}F_n^- \rightarrow [(CH_3O)_2PO]^- + CHCl_{3-n}F_n \quad (n = 0, 1, 2) \quad (11)$$

Another alternative possibility that should be evaluated is the proton abstraction from the hydroxyl group of monomethyl phosphonate **3**, which according to the above considerations, should be present in the system in equimolar quantity with the corresponding carbanions.

$$(CH_3O)(HO)P(O)H + CCl_{3-n}F_n^- \rightarrow [(CH_3O)PHOO]^- + CHCl_{3-n}F_n \quad (n = 0, 1, 2) \quad (12)$$

For this alternative pathway, the monomethyl phosphonate anion is formed together with the corresponding hydrochlorofluorocarbon, thereby closing an alternative three-step catalytic cycle that is described in further detail in the last section of this paper.

Table VIII. Calculated Energies (kcal/mol) of the Reaction between Dimethyl Phosphonate (1) and Chloro- and Fluoro-Substituted Methanide Anions: $(CH_3O)_2P(O)H + CCl_{3-n}F_n^- \rightarrow [(CH_3O)_2PO)^- + CHCl_{3-n}F_n$

n	SCF	MP2	MP2 + ZPE
0	−6.1	−20.0	−19.1
1	−8.8	−21.8	−20.4
2	−15.9	−24.6	−22.6

Table IX. Calculated Energies of the Reaction between Monomethyl Phosphonate (3) and Chloro- and Fluoro-Substituted Methanide Anions: $(CH_3O)(HO)P(O)H + CCl_{3-n}F_n^- \rightarrow [CH_3OPHOO]^- + CHCl_{3-n}F_n$

n	SCF	MP2	MP2 + ZPE
0	−29.9	−39.8	−38.0
1	−32.6	−41.5	−39.2
2	−39.8	−44.2	−41.4

The data in Tables VIII and IX summarize the energy evaluations of the two pathways that correspond to eqs 11 and 12. A comparison of the data indicates that the abstraction of a proton from the hydroxyl group of the monomethyl phosphonate is the preferred pathway. The energy difference as compared to the other alternative process (eq 11) is *ca.* −19.0 kcal/mol, and it does not depend on the fluorine content of the carbanion. This energy preference is also clearly supported by the computed relative acidities and basicities (Tables V and VI) of the phosphorus-containing species in eqs 11 and 12. Thus, in terms of base–acid interactions, the proton abstraction step from monomethyl phosphonate **3** (eq 12) is more favorable than from dimethyl phosphonate **1**, because **3** is the stronger acid. In addition, the anion of monomethyl phosphonate, which is the conjugated base in eq 12, is a weaker base than is the anion of monomethyl phosphite **8** that is formed in eq 11.

Total Calculated Energy of the Atherton–Todd Reaction of Dimethyl Phosphonate with Different Chloro- and Fluorosubstituted Methanes. From the computed total energies of the reactants and products (Tables I and II) for the reaction between dimethyl phosphonate and a chlorofluorocarbons $CCl_{4-n}F_n$, and taking into account the zero-point vibrational energy corrections, we can calculate the total energy for the overall reaction given in eq 13. The results of these calculations are summarized in Table X.

Table X. Calculated Energies (kcal/mol) of the Reaction between Dimethyl Phosphonate (1) and Chloro- and Fluoro-Substituted Methanes: $(CH_3O)_2P(O)H + CCl_{4-n}F_n \rightarrow (CH_3O)_2P(O)Cl + CHCl_{3-n}F_n$

n	SCF	MP2	MP2 + ZPE
0	−34.7	−23.2	−32.7
1	−30.6	−20.3	−17.7
2	−27.4	−18.5	−16.1

$$(MeH)_2P(O)H + CCl_{4-n}F_n \rightarrow (n = 0, 1, 2)$$
$$(MeO)_2P(O)Cl + CHCl_{3-n}F_n \quad (13)$$

These data show that the free energies of reaction 13 for the series of compounds CCl_4, CCl_3F, and CCl_2F_2 are −32.7, −17.7, and −16.1 kcal/mol, respectively, on MP2 calculational levels, including the ZPE corrections. This theoretical result for the reaction thermodynamics is consistent with the results of our recent experimental study on the reactivity of dimethyl phosphonate toward different chlorosubstituted methanes, for which the following relative reactivity order with dialkyl phosphonates has been established: $CCl_4 > CCl_3F > CCl_2F_2$.[13] One possible explanation for this order of reactivity arising from our calculations is that it is determined by the reaction step which includes the formation of the dialkyl chlorophosphonate. As discussed earlier, this step involves chlorine abstraction from the corresponding chloro- and fluorosubstituted methane by the anion of dimethyl phosphite **8**. Our results are also in agreement with those of Todd and Atherton, which show that the relative reactivity of chlorofluorocarbons with dialkyl phosphonates decreases as the number of fluorine substituents on the carbon increases.[2b]

Summary

Our calculations support the mechanism shown in Scheme III for the amine promoted Atherton–Todd reaction.

Here the initial step is the reaction of the amine with the dialkyl phosphonate to form the corresponding monoalkylphosphonium salt. The subsequent three steps form the catalytic cycle that leads to product formation. The anion of the monoalkyl phosphonate, acting as a base, first deprotonates the dialkyl phosphonate to generate the reactive dialkyl phosphite anion. In the subsequent step, which is the same as that shown in the mechanism presented in Scheme I, the dialkyl chlorophosphonate is formed along with the trichloromethanide anion. The catalytic cycle is completed with the reaction of this trichloromethanide anion with monomethyl phosphonate to form chloroform and the monoalkylphosphonate anion. The monoalkylphosphonate anion can then react with a further molecule of dialkyl phosphonate in a new catalytic cycle. The major reasons for us to reject the earlier proposed mechanism of the Atherton–Todd reaction is the absence of a critical point along the N—H–P reaction coordinate. In addition to this computational result, numerous experimental observations concerning the alkylation reaction[7,8] provide further support for this conclusion. One such observation is the fact that the alkylated products thus obtained are themselves catalysts in the above reaction.[8] Although the overall alkylation

Scheme III

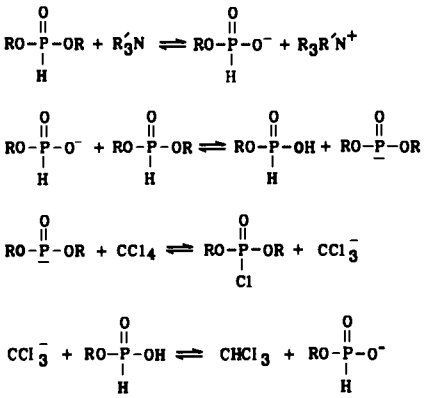

reaction between dimethyl phosphonate and ammonia is calculated to be endothermic in the gas phase, the formation of the contact hydrogen-bonded ion pair ADD1 between the reaction products is indicitive of the role of both hydrogen bonding and solvation effects in the stabilization of alkylation products in solution.

Another key result of this theoretical study is the fact that our calculations support the suggestion that the monomethyl phosphonate anion is the actual base, which then deprotonates dialkyl phosphonate to form the highly reactive dimethyl phosphite nucleophile. Since the formation of this nucleophile is a common step in amine-catalyzed reactions of dialkyl phosphonates that involve cleavage of the P–H bond,[6] we consider the deprotonation to be a two-step process rather than a single step process involving direct deprotonation of the dialkyl phosphonate by the amine.

The calculated high activation energy for the noncatalyzed tautomerization of dialkyl phosphonate to dialkyl phosphite indicates that it is probably a base- or an acid-catalyzed process. In the case of the phosphonate anion being the base, the reactive three-coordinate anion is formed before the tautomerization step is completed. Thus it is not necessary to invoke the presence of catalytic quantities of the dialkyl phosphite tautomeric form in order to explain the amine activation of dialkyl phosphonates in this family of reactions that result in P–H bond cleavage.

The computed total energy for the overall reactions of dimethyl phosphonate with different chlorofluoromethanes decreases with increasing fluorine contact, which is in good agreement with our experimental results.[22] This reactivity order correlates well with the calculated reaction energies for the chlolrue abstraction from chlorofluoromethanes by olimethyl phosphite anion, which is one of the key steps in the Atherton–Todd reaction mechanism.

Acknowledgment. We thank Dr. Toon Cheam for access to the GAUSSIAN 90 system. We thank the Tulane Computer Services for providing computer resources. We thank the Center for Bioenvironmental Research at Tulane University and the National Science Foundation (INT 9113923) for financial support.

Supplementary Material Available: Tables of computed structural data for compounds **1–6** and figures representing conformers for compounds **2**, **5**, **6**, **7**, **9**, and **10** (12 pages). Ordering information is given on any current masthead page.